

Supporting Information

Visualization of crystal plane selectivity for irreversible phase

transition in MnO@C anode

Tong Zhou,^{†,a} Liang Chang,^{†,a} Weiqin Li,^b Chao Li,^{*,a} Wenjuan Yuan,^{*,a} Cuihua An^{*,a}
and Jun Luo^a

^aTianjin Key Laboratory of Advanced Functional Porous Materials, Institute for New Energy Materials and Low-Carbon Technologies, School of Materials Science and Engineering, Tianjin University of Technology, Tianjin 300384, P.R. China.

^bKey Laboratory of Advanced Energy Materials Chemistry (Ministry of Education), Renewable Energy Conversion and Storage Center, College of Chemistry, Nankai University, Tianjin, 300071 P. R. China.

Corresponding Author

*Correspondence and requests for materials should be addressed to chao_li@tjut.edu.cn; yuanwj@email.tjut.edu.cn; ancuihua@tjut.edu.cn

Experimental Details

Fabrication of electron microscopy samples

The preparation of MnO@C and the fabrication of the coin cell samples are reported in our previous study.¹² Galvanostatic charge-discharge (GCD) measurements were performed on a LAND (CT2001A) battery test system. The MnO@C anodes at various charging/discharging states were obtained, which were used as electron microscopy samples.

Characterization

The sample crystallinity was determined by x-ray diffraction (XRD, SmartLab 9 KW) using Cu K α radiation. The Li content was determined via x-ray photoelectron spectroscopy (XPS) with an ESCALAB 250Xi spectrometer (Thermo Scientific). The transmission electron microscopy (TEM) images and selected-area electron diffraction (SAED) patterns were captured using a field emission transmission electron microscope (FEI Talos F200X) with an acceleration voltage of 200 kV. The atomic-resolution high-angle annular dark field (HAADF) images and annular bright field images (ABF) were captured using an aberration corrected scanning transmission electron microscope (FEI Titan Cubed Themis G2 300) operating at 200 kV. The scanning electron microscopy (SEM) images were obtained using an FEI Verios 460L microscope.

Supplementary Figures

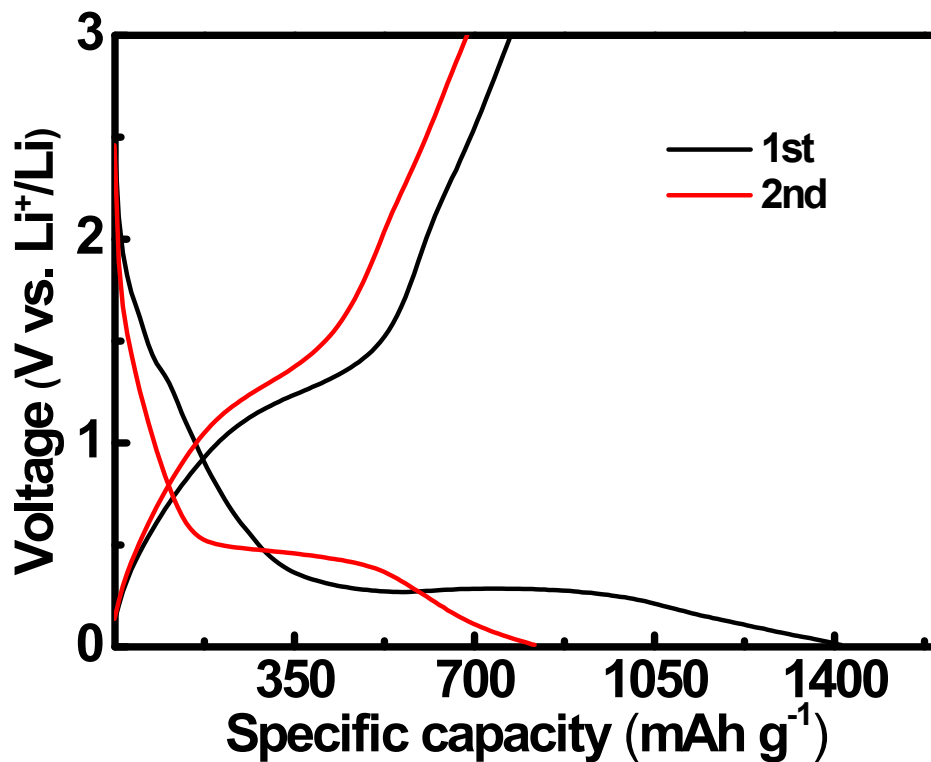


Fig. S1 GCD curve of MnO@C anode.

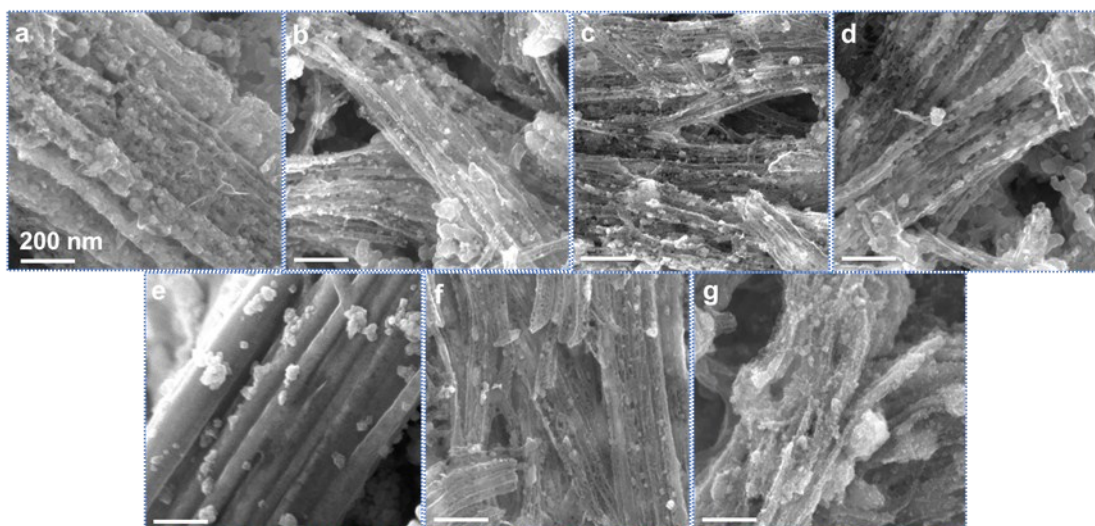


Fig. S2 SEM images of MnO@C electrode under different states. a: Sample 1. b: Sample 2. c: Sample 3. d: Sample 4. e: Sample 5. f: Sample 6. g: Sample 7.

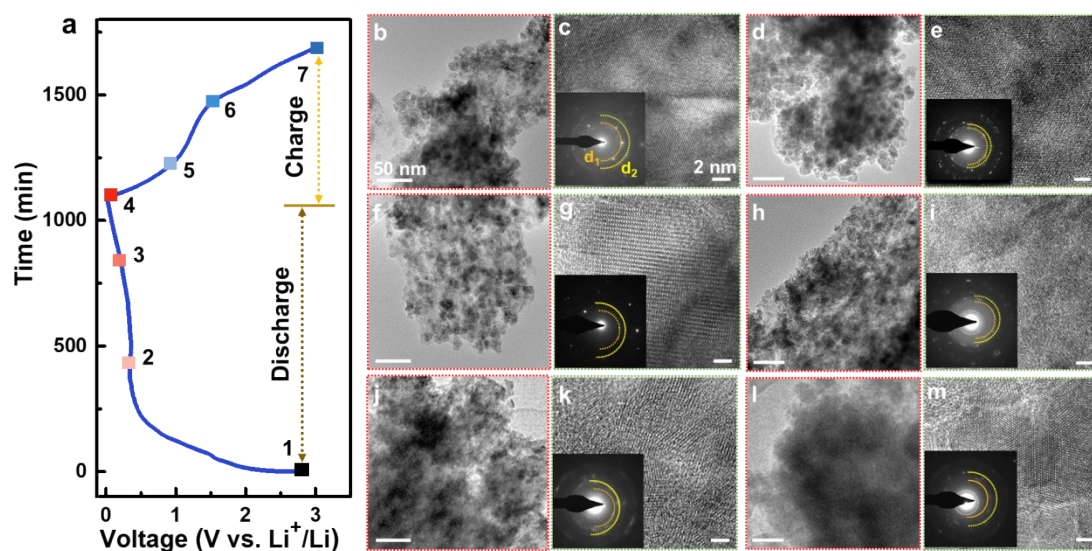


Fig. S3 HRTEM images of MnO@C anodes during lithiation/delithiation process. (a) GCD curves of MnO@C anode during first cycle. (b–m) Low-magnification HRTEM images of Samples 2 (b, c), 3 (d, e), 4 (f, g), 5 (h, i), 6 (j, k), and 7 (l, m). The insets depict the SAED patterns of the corresponding HRTEM images.

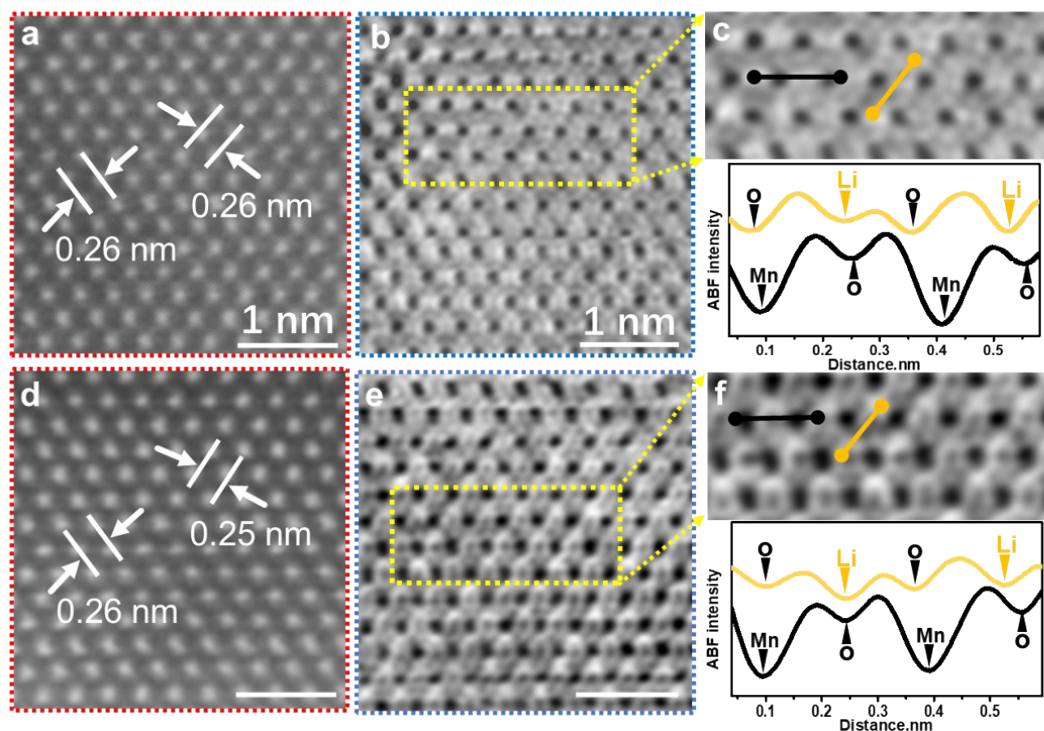


Fig. S4 HAADF and ABF images of MnO@C electrode. (a–c) Sample 3. (d–f) Sample 5. (c, f) Enlarged ABF images, with the intensity profiles along the Mn-O and Li-O pairs indicated by black and yellow lines, respectively.

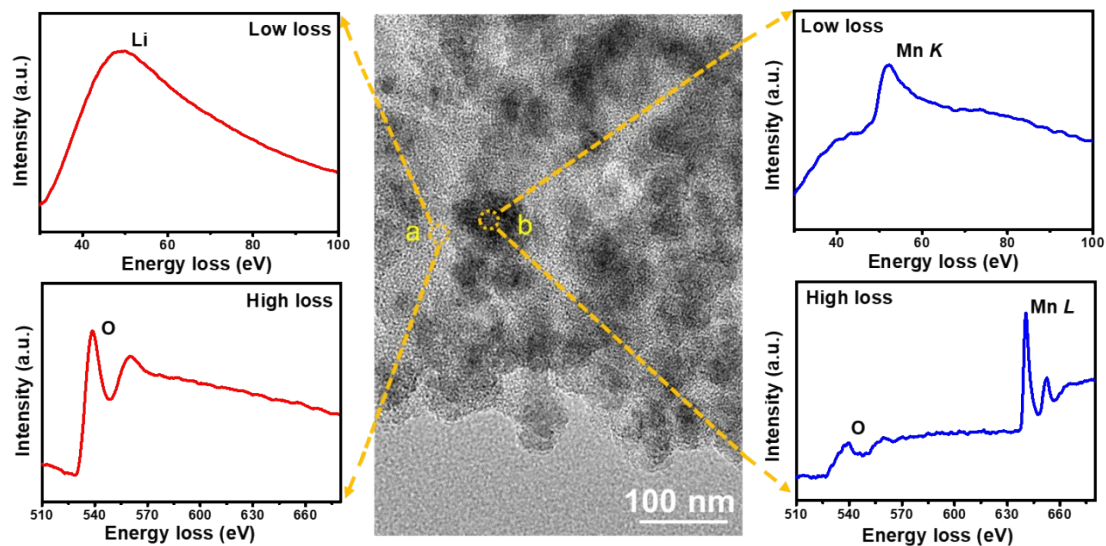


Fig. S5 EELS of Sample 4. (a) EELS of surface area. (b) EELS of bulk area.

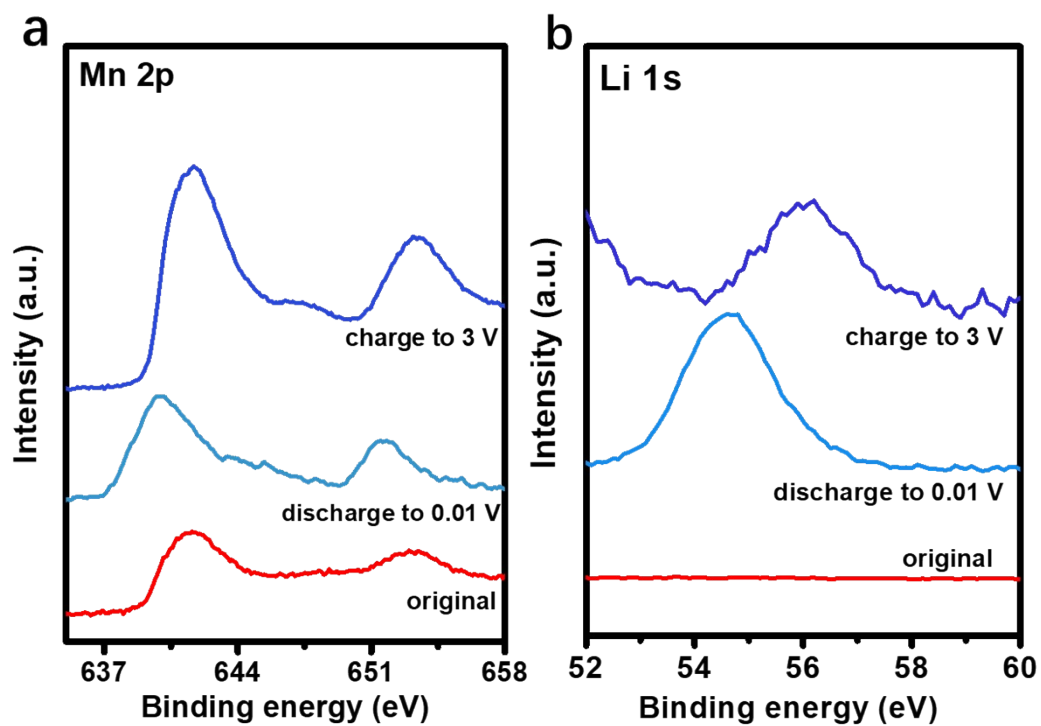


Fig. S6 XPS patterns for Mn 2p (a) and Li 1s (b) of Samples 1, 4, and 7.

Table S1 Interplanar spacing of Samples 1–7 obtained via SAED.

| Sample | Interplanar spacing d (nm) | |
|--------|----------------------------|------------|
| | $d_1(200)$ | $d_2(220)$ |
| 1 | 0.222 | 0.157 |
| 2 | 0.263 | 0.178 |
| 3 | 0.265 | 0.220 |
| 4 | 0.256 | 0.220 |
| 5 | 0.257 | 0.212 |
| 6 | 0.258 | 0.209 |
| 7 | 0.257 | 0.156 |

Table S2 Li content in Samples 1–7 at different etching depths determined using XPS.

| Sample | Li content (wt%) | | |
|--------|------------------|-------|-------|
| | 0 nm | 20 nm | 40 nm |
| 1 | 0 | 0 | 0 |
| 2 | 23.55 | 30.53 | 31.37 |
| 3 | 26.69 | 33.17 | 34.66 |
| 4 | 27.09 | 33.55 | 34.73 |
| 5 | 24.03 | 30.26 | 32.05 |
| 6 | 18.9 | 29.47 | 30.47 |
| 7 | 5.15 | 5.19 | 5.82 |

The Li content in bulk was quantitatively analyzed by performing XPS measurements at different etching depths, as presented in Table S2. The variation trend of Li was the same at all the depths. At the beginning of discharge, Li quickly entered the electrode and reached its peak when discharged to 0.01 V. As charging progressed, the formation of the SEI on the surface suppressed Li diffusion; this resulted in sluggish Li extraction kinetics in the MnO@C structure, which caused the Li content to decrease slowly. At the end of charging, irreversible transformation of the MnO@C structure occurred, leading to a rapid decline in Li content as the structure deteriorated. The test result at 40 nm was considered for analysis. Approximately 34.73% of Li was embedded at the end of the discharge state, while 5.82% remained at the end of the charging state.

Reference

12. W. Li, C. An, H. Guo, J. Sun, M. Wang, Y. Li, L. Jiao and Y. Wang, *ACS Sustainable Chem. Eng.*, 2018, **7**, 139-146.